

## ENVIRONMENTAL FACTORS AFFECTING CORROSION OF SABIC MILD STEEL IN ACID CHLORIDE SOLUTIONS

A. G. Gad Allah\*, M. A. Al-Khalidi and R. K. Al-Bilali

Chemistry Department, Girls' College of Science,

P.O.Box 838, Dammam, Saudi Arabia

(Received 26<sup>th</sup> Sept. 2006; Accepted 16<sup>th</sup> Dec. 2006)

تناول البحث دراسة السلوك التآكلي لصلب سابك المعتدل (أحد منتجات صناعات الصلب السعودية) في محاليل الكلوريد الحمضية تحت ظروف بيئية مختلفة من تركيز الحمض، درجة حرارة وحالة المحلول باستخدام قياسات الفقد في الوزن، الجهد، المعاوقة الكهربائية والاستقطاب البوتنوديناميكي، بالإضافة إلى الفحص الميتالورجي لأسطح العينات تحت الاختبار. أوضحت النتائج زيادة معدل التآكل مع زيادة تركيز الحمض، حرارة المحلول وزمن الغمر. كما أن عملية التآكل تتأثر بظروف الاستقطاب أكثر من تأثرها بظروف الدائرة المفتوحة حيث أنها تسرع من عملية التآكل. أيضاً لا تتأثر خطوات التتابع الميكانيكي للعمليات الكهروكيميائية الأنودية والكاثودية مع تركيز الحمض ودرجة الحرارة وإنما يزداد معدل سرعتها بزيادة. كما أن حالة المحلول تعطي تأثير ضعيف على عملية التآكل. تم حساب طاقة التنشيط والتي تساوي تقريباً  $57.4 \text{ kJ/mol}$ . أوضحت دراسة الفحص الميكروسكوبي لأسطح العينات وجود نقر خلال طبقة الأكسيد المتكونة على السطح يعتمد عددها وعمقها على تركيز الحمض ودرجة حرارة المحلول.

The corrosion behavior of Sabic mild steel in HCl solutions was studied under different environmental factors such as acid concentration, solution temperature and state, using weight loss, open – circuit potential, EIS and potentiodynamic polarization measurements, and optical microscopy. The rate of corrosion increases with increasing acid concentration, solution temperature and immersion time. Also, the corrosion process is affected by polarization than open-circuit conditions, i.e. accelerate the corrosion process. The mechanistic sequences of each of the cathodic and anodic electrochemical processes are uninfluenced with acid concentration and temperature but their rates are increased with increasing both factors. Also, the solution states showed nearly a minor effect on the corrosion process. The activation energy is calculated and equal  $\approx 57.4 \text{ kJ/mol}$ . The SEM studies showed pits along the oxide film formed on the surface as a result of corrosive action of ions, its number and propagation depend on acid concentration and solution temperature.

### INTRODUCTION

The study of corrosion of iron and mild steel is a matter of tremendous theoretical and practical investigations under different conditions and as such has received a considerable amount of interest [1-5]. Acid solutions widely used in industrial acid pickling, acid descaling and oil-well acidizing, required addition of corrosion inhibitors in order to restrain their corrosion attack [6-9]. The ability of an inhibitor to provide corrosion protection depends largely upon the interactions between metal surface and inhibitor

which change with the actual corrosion conditions. An accurate knowledge about the corrosion behavior of the metal not only helps to identify the prevailing form of corrosion but also for prescription of appropriate anti-corrosion measures.

Most of the prevailing corrosion mechanism theories are based either on the catalyzed mechanism of Heusler or the consecutive mechanism of Bockris, and either mechanism can be followed depending on the surface microstructure [1,10]. In the presence of chloride ions which is particularly one of the most

\* To whom all correspondence should be addressed

aggressive and accelerate corrosion tend to be strongly adsorbed on the metal surface and accordingly changes the dissolution mechanism. Keddam *et al* have investigated the dissolution mechanism by EIS, the impedance diagrams were interpreted by a reaction model depending on the surface structure [11].

In the present work the corrosion behavior of Sabic mild steel in acid chloride solutions has been investigated under different environmental conditions of solution concentration, nature of solution and temperature and also under open-circuit and imposed voltage using weight loss, open-circuit potential and impedance (EIS), potentiodynamic polarization measurements and morphological surface investigation. An understanding of such behavior is necessary before extension on the corrosion inhibition studies in acid chloride solutions containing carbamide and thiocarbamide derivatives which will be done latter.

## EXPERIMENTAL

The mild steel used was produced by Iron & Steel Saudian Company, one of Sabic Groups of Companies, Industrial Gobial, K.S.A. It had the following composition (in percentages)

| C     | Si   | Mn    | P      | S       | Al     | N      |
|-------|------|-------|--------|---------|--------|--------|
| 0.058 | 0.01 | 0.381 | 0.0088 | 0.01015 | 0.0382 | 0.0047 |

The preparation of the electrodes and the specimens for weight loss, open-circuit potential and impedance (EIS), and polarization measurements were described previously [12,13]. All measurements were carried out at a constant room temperature of 25°C. Potential and EIS measurements were performed using Gill AC instrument (ACM Instruments, GB) The input signal amplitude was usually 10 mV peak to peak in the frequency domain from 0.01 Hz to 30 kHz measurements were interfaced to a computer. All solutions were prepared from analytical grade chemicals using triply distilled water.

Deaeration of solutions was affected with purified nitrogen gas which allowed to pass through the solution for about 30 minute before the experiment and over the solution during the experiment. The solution stirring was performed by bubbling N<sub>2</sub> gas through the solution via very slow stream rate of nitrogen in addition to the first deaeration.

For morphological investigations the samples were prepared and treated as described previously [12]. The samples were examined before and after corrosion measurements using optical microscope with CCD IRIS camera, Zeiss-Japan.

## RESULTS AND DISCUSSION

### 1. Effect of HCl concentration :

#### 1.1. Weight loss studies:

Fig. 1 shows the variation of corrosion rate,  $R_{\text{corr}}$  calculated from weight loss measurements with concentration of HCl within the range of 0.1 M to 2.0 M at 25°C. As can be seen the variations depend on acid concentration and become small at low concentrations, <1.0 M, as compared with higher concentrations, > 1.0 M. Fig. 2 presents the kinetic studies in the terms of weight loss per unit area,  $\Delta W$ , with time for different concentrations of acid . As obvious from figure the loss in weight is linearly increased with time and follows the following equation [14]:

$$\Delta W = kt + C \quad (1)$$

Where k and C are constants depend on the nature and concentration of electrolyte used and also on solution state and temperature and normally the electrode type. The constancy of the slope values indicates that the nature of products of corrosion processes for Sabic mild steel in HCl solutions are similar irrespective of acid concentration and duration of corrosion process.

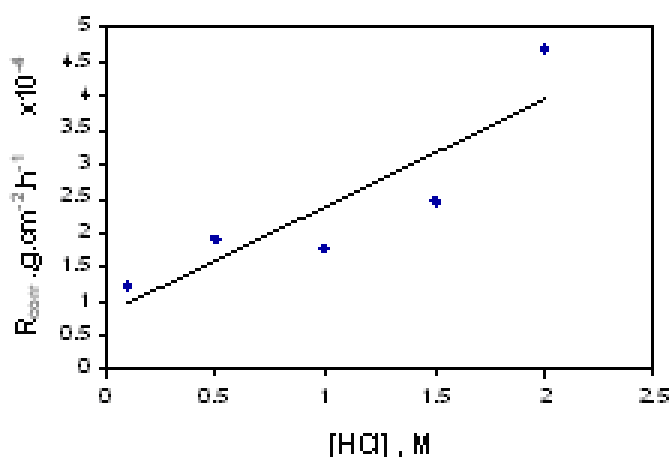


Fig. 1:  $R_{\text{corr}}$ , determined from weight loss measurements versus [HCl] for Sabc mild steel at 25°C.

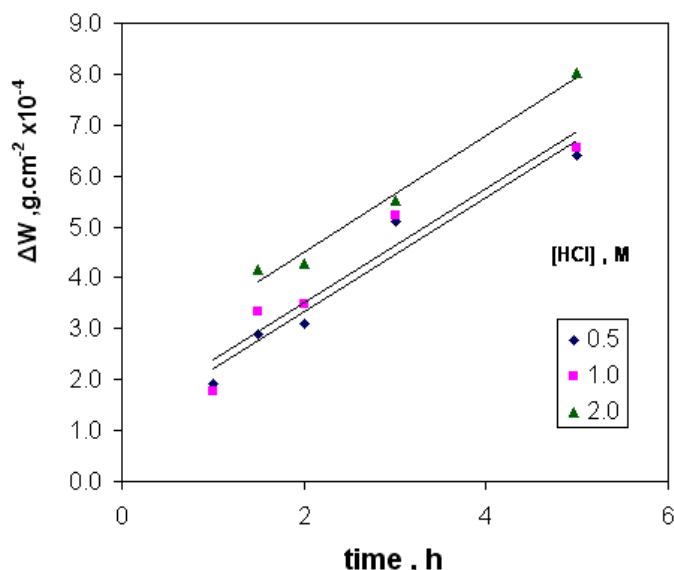


Fig. 2: Kinetic studies of corrosion rate, in terms of weight loss,  $\Delta W$ , versus time for Sabc mild steel in HCl solutions of different concentrations at 25°C.

## 1.2. Open-circuit potential (OCP) measurements:

Fig. 3 shows the variation of open-circuit potential,  $E$ , of Sabc mild steel electrode measured versus SCE with time in naturally aerated HCl solutions of different concentrations at 25°C. As observed from figure for all solutions the potential drifts with time initially to more negative values then to more positive values through a transition or minimum potential,  $E_{\text{min}}$ ,

and finally to steady state. Generally, the rate of potential change with time, transition potential ( $E_{\text{min}}$ ) and the time required to attain steady state are acid concentration dependent. Plots of each of  $E_{\text{min}}$  and  $E_{\text{ss}}$  with [HCl] are obvious in Fig. 4a and b. As can be seen the effect of acid concentration are reflected on the time required to attain  $E_{\text{min}}$  which becomes small for concentrated acid ( $\approx 1$  min for 1.5 M) and relatively large dilute ones ( $\approx 6.1$  min for 0.1 M), cf Fig 4a. Furthermore,  $E_{\text{min}}$  shifts to more positive values with increasing

[HCl]. Such shifts reflect that the electrode surface is subjected to corrosion processes, i.e. simultaneous occurrence of cathodic and anodic processes at the electrode surface [15]. It would appear reasonable therefore to characterize the potential observed as being a mixed one.

On the other hand,  $E_{ss}$  drifts to more positive values with increasing [HCl], cf. Fig. 4b which

indicates that the anodic process being continually stifled up. The amount of potential shift,  $\Delta E_{shift}$ , between  $E_{min}$  and  $E_{ss}$ , increases with increasing acid concentration ( $\Delta E_{shift} = 0.035$  V for 0.1 M and 0.04 V for 1.5 M HCl). So, the values of potential shifts show to what extent the anodic oxide film formed on the electrode surface is greatly affected with acid concentration.

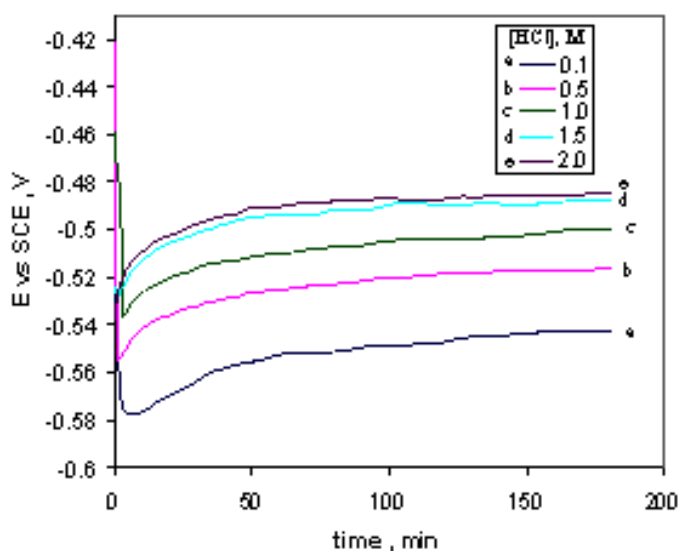


Fig. 3: Variation of open-circuit potential,  $E$  vs SCE, for Sabc mild steel electrode with time in HCl solutions of different concentration at 25°C.

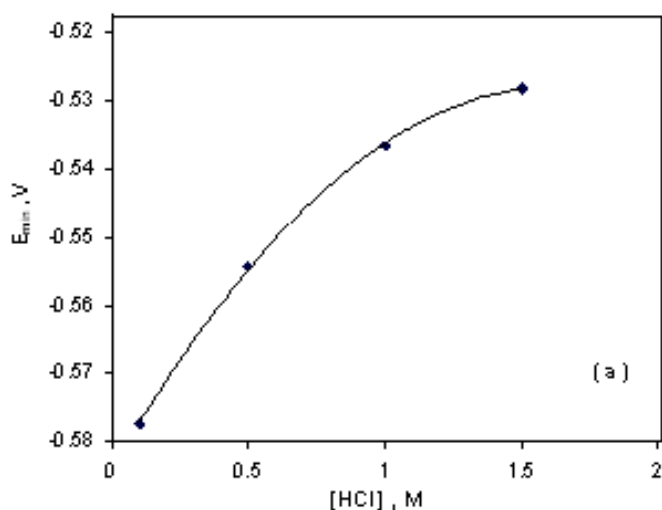


Fig. 4a:  $E_{min}$  versus [HCl] at 25°C for Sabc mild steel electrode.

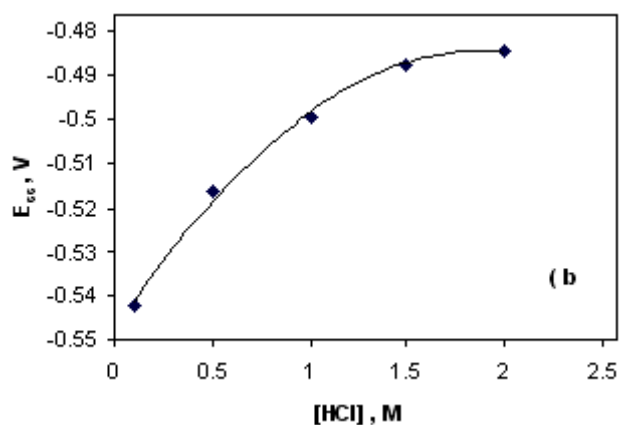


Fig. 4b:  $E_{ss}$  versus [HCl] at 25°C for Sabc mild steel electrode.

EIS measured at steady state after 3 hours immersion in HCl solutions of different concentrations are presented in Nyquist plots as in Fig. 5. The complex plane represents an incomplete semicircle, whose diameter increases with decreasing [HCl]. The exact diameter of the depressed semicircle was determined to estimate the value of polarization resistance,  $R_p$  of the oxide layer formed on the electrode surface [16]. Fig. 6a illustrates the values of  $R_p$  versus [HCl] which decreases with increasing [HCl]. It indicates that the concentration of active species like  $H^+$  ions increases with increasing acid concentration at electrode surface which lead to accelerate the charge transfer at the electrical

double layer, as a consequence  $R_p$  decreases. Also, it is important to note that the relation between semicircle diameter and solution concentration is governed by the dissolution acid effect.

The double layer capacitance,  $C_{dl}$ , determined from the resonance frequency  $\omega_{max}$  at the maximum value of  $Z''$  ( $C_{dl} = 1/\omega_{max} R_p = 1/2\pi f_{max} R_p$ ) [17], and its relation with [HCl] is shown in Fig. 6b. As can be seen  $C_{dl}$  increases with increasing the acid concentration which indicates that the oxide film thickness decreases with the ascending of the acid concentration ( $C_{dl} \propto 1/d$  where  $d$  is the oxide film thickness). Such results confirm the preceding conclusions derived from the other measurements.

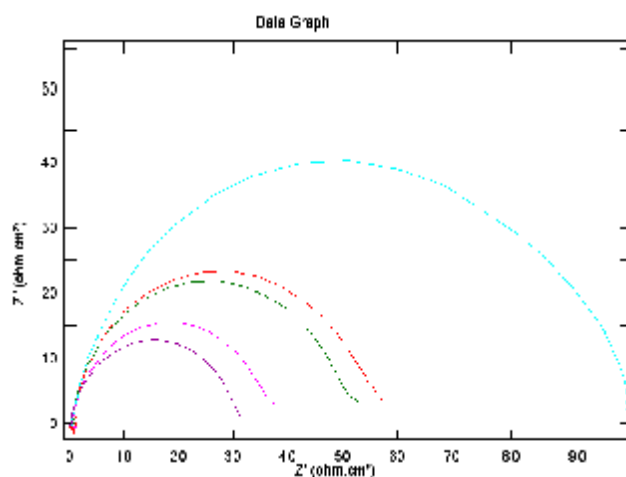


Fig. 5: EIS measurements presented in Nyquist plot for Sabc mild steel electrode in HCl solutions of different concentrations at 25°C

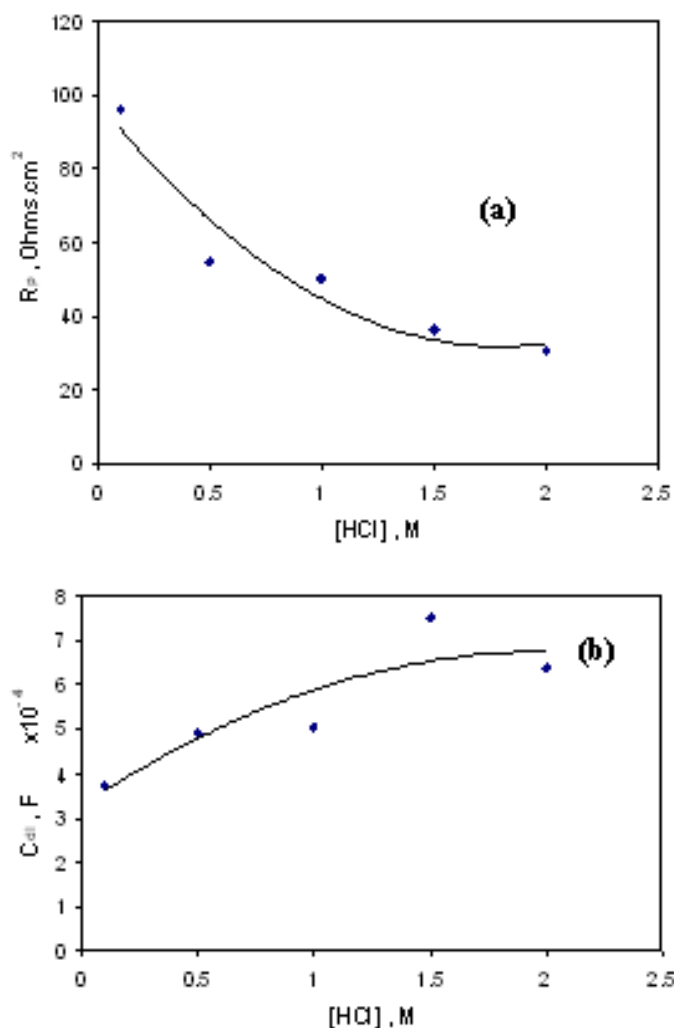


Fig. 6: (a)  $R_p$  versus [HCl] for Sabic mild steel electrode at 25° (b)  $C_{dl}$  versus [HCl] for Sabic mild steel electrode at 25°C.

### 1.3. Potentiodynamic polarization measurements:

Polarization curves of the Sabic mild steel electrode in HCl solutions of different concentrations at 25 °C using scanning rate of 100 mV/min within potential range of –800 mV to –200 mV are shown in Fig. 7. As obvious the cathodic and anodic portions of the polarization curves are nearly parallel to each other

irrespective of acid concentration, indicating that the electrochemical processes were occurred under activation controlled and their mechanism were similar. Values of associated electrochemical parameters such as corrosion potential,  $E_{\text{corr}}$ , corrosion current,  $I_{\text{corr}}$ , cathodic and anodic Tafel slopes ( $b_c$  and  $b_a$ ), polarization resistance ( $R_p = b_a b_c / 2.303 I_{\text{corr}} (b_a + b_c)$ ) are presented in Table 1.

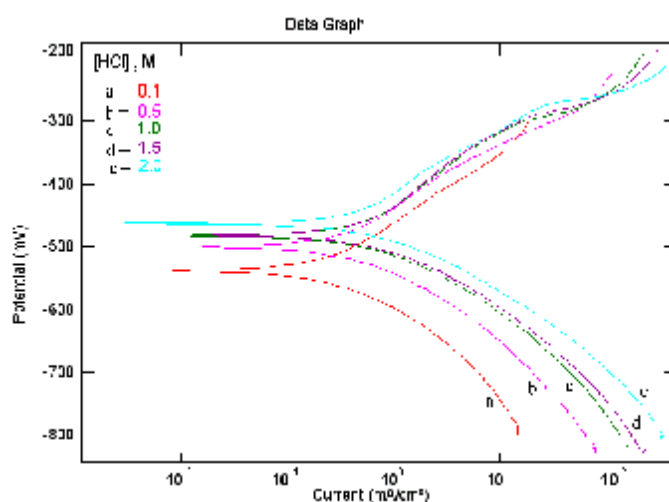


Fig. 7: Potentiodynamic polarization curves (cathodic and anodic) for Sabic mild steel electrode in HCl solutions of different concentrations at 25°C using scanning rate of 100 mV/min.

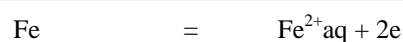
Table 1: Polarization parameters for Sabic mild steel electrode in HCl solutions of different concentrations at 25°C.

| [HCl]<br>M | $E_{\text{corr}}$<br>V | $I_{\text{corr}}$<br>$\text{mA}\cdot\text{cm}^{-2}$ | $b_c$<br>mV | $b_a$<br>mV | $R_p$<br>$\text{Ohm}\cdot\text{cm}^2$ |
|------------|------------------------|---|-------------|-------------|---------------------------------------|
| 0.1        | -0.534                 | 0.13  | 91.67       | 95.04       | 154.87                                |
| 0.5        | -0.489                 | 0.17  | 92.06       | 95.32       | 123.4                                 |
| 1.0        | -0.467                 | 0.24  | 92.16       | 95.51       | 83.92                                 |
| 1.5        | -0.466                 | 0.42  | 93.05       | 95.81       | 48.52                                 |
| 2.0        | -0.463                 | 0.56  | 93.57       | 95.90       | 36.77                                 |

As it can be seen from the polarization results, the  $E_{\text{corr}}$  shifts to more positive values and  $I_{\text{corr}}$  increases with increasing the acid concentration. Such data illustrate the corrosive action of HCl solutions under the applied potential as compared to open-circuit conditions ( $E_{\text{ss}} = -0.542, -0.516, -0.499, -0.488, -0.484$  V for 0.1, 0.5, 1.0, 1.5 and 2.0 M HCl, respectively). Also, it indicates the effect of adsorbed chloride ions on the electrode surface which become more effective in case of polarization and lead to appearance of pits on the sample surface, its spreading depends on acid concentration.

On the other hand, the constancy of slope values ( $b_c = 92$  mV and  $b_a = 95$  mV) irrespective

of HCl concentration indicate that the mechanistic sequence of each of the cathodic and anodic electrochemical processes are similar. On view of the previous pertinent literatures together with the obtained data [1, 4, 19], one can assume the following sequences for the anodic dissolution reaction as follows:



The most probable cathodic reaction associated with the cathodic polarization curve is hydrogen reduction according to the following overall reaction:



Generally, under potentiodynamic polarization conditions the presence of  $\text{Cl}^-$  ions leads to corrosive action and formation of pits, its extent depend on acid concentration. Such results are preliminarily observed on surface of Sabic mild steel samples.

In the same way, comparison of the  $R_p$  calculated from polarization curves, Table 1, with that obtained from EIS measurements ( $R_p = 96.05, 54.88, 50.11, 36.27$  and  $30.49 \Omega.\text{cm}^2$  for 0.1, 0.5, 1.0, 1.5 and 2.0 M HCl, respectively) indicates that polarization conditions give a higher  $R_p$  values. As mentioned previously the data of  $R_p$  reflect the corrosive action of acid where  $R_p$  decrease with increasing the acid concentration from one hand and increases under polarization conditions on the other hand.

## 2. Effect of Solution State:

The question arises here is to what extent the oxygen of the solution affect the electrochemical processes occurring on the Sabic mild steel electrode in HCl solutions under open-circuit and polarization conditions? The answer of such question comes from measurements presented in Fig. 8a-c. As seen from variation of open-circuit potential with time Fig. 8a, a small potential

change to less negative values was demonstrated in 2.0 M HCl solutions  $\text{N}_2$ - deaerated, stagnant or stirred, than that of naturally aerated solution. Also, the potential transition,  $E_{\text{min}}$ , was recorded in  $\text{N}_2$ - deaerated solution indicating that the stirring process affects the double layer containing the adsorbed anions and consequently the formed oxide film.

The above finding seems to accord also with those obtained by EIS and presented in Fig. 8b. As can be seen the Nyquist complex plane retain its pattern as incomplete semicircle whose diameter depends on solution state, it increases in case of  $\text{N}_2$ -deaerated 2.0 M HCl solutions, stagnant and stirred. The values of  $R_p$  are equal to 43.11 and 41.33  $\Omega.\text{cm}^2$  in case of stagnant and stirred  $\text{N}_2$ -deaerated solutions, respectively and 30.49  $\Omega.\text{cm}^2$  in naturally aerated solution. Since  $R_p$  is universally proportional to the thickness of the formed oxide film [17], therefore, a relatively more thick film is formed in  $\text{N}_2$ -deaerated stagnant and stirred than that in naturally aerated solution. It is important to illustrate that the corrosion of Sabic mild steel proceeds via cathodic reduction of  $\text{H}^+$  ions mainly.

As obvious from potentiodynamic polarization curves, Fig. 8c the state of solution has generally no effect on Tafel plots, indicating that the cathodic and anodic electrochemical processes were occurred under activation controlled. Values of associated electrochemical parameters,  $E_{\text{corr}}$ ,  $I_{\text{corr}}$ ,  $b_c$ ,  $b_a$  and  $R_p$  are presented in Table 2.

**Table 2: Polarization parameters for Sabic mild steel electrode in 2.0 M HCl solutions under different states at 25 °C.**

| Solution State                       | $E_{\text{corr}}$<br>V | $I_{\text{corr}}$<br>$\text{mA.cm}^{-2}$ | $b_c$<br>mV | $b_a$<br>mV | $R_p$<br>$\Omega.\text{cm}^2$ |
|--------------------------------------|------------------------|--|-------------|-------------|-------------------------------|
| Naturally- aerated                   | -0.463                 | 0.56                                     | 95          | 94          | 36.77                         |
| Stagnant $\text{N}_2$ -<br>deaerated | -0.465                 | 0.40                                     | 90          | 95          | 50.36                         |
| Stirred $\text{N}_2$ -<br>deaerated  | -0.465                 | 0.42                                     | 90          | 95          | 47.65                         |

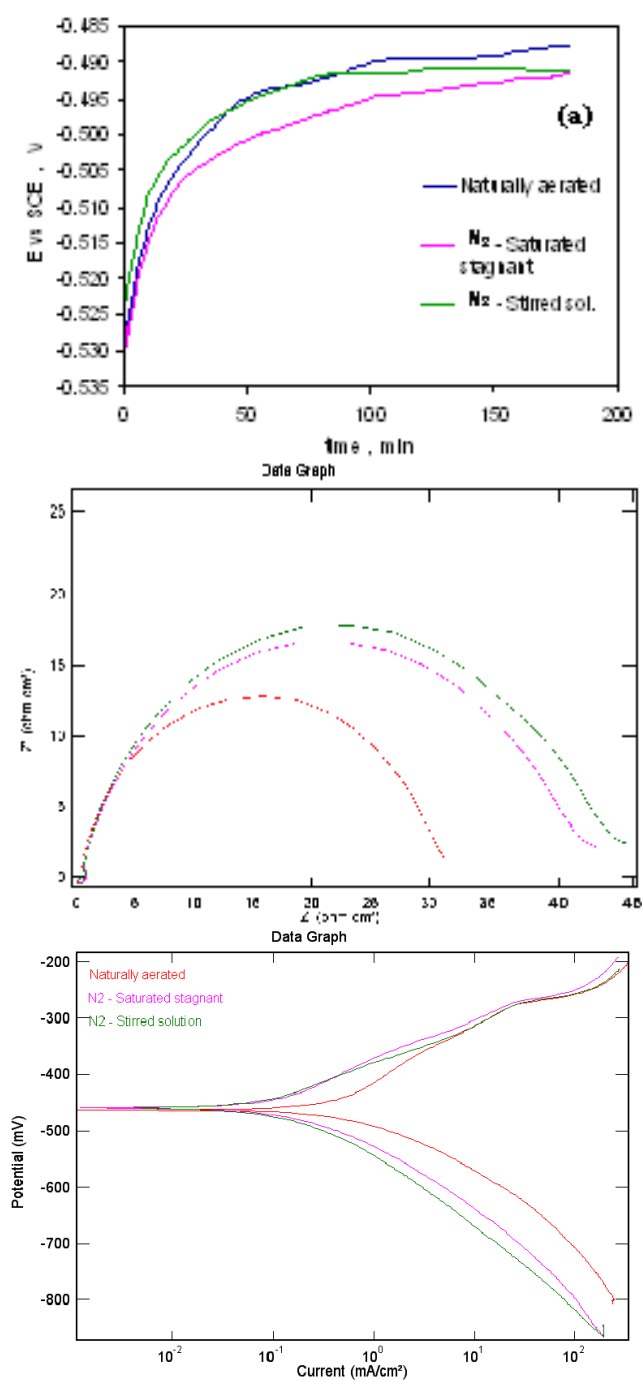


**Fig. 8:** Variation of open-circuit potential,  $E$  vs SCE, with time (a), EIS measurements presented in Nyquist plot (b) and potentiodynamic polarization curves (cathodic and anodic) (c) for Sabc mild steel electrode in 2.0 M HCl solutions under different states at 25°C.

A careful consideration of the data gathered in Table 2 reveals the following points:

1. The minor effect of solution state on  $E_{\text{corr}}$  under different conditions as compared with steady state open-circuit potential ( $E_{\text{ss}} = -0.484, -0.486, \text{ and } -0.487 \text{ V}$  for naturally aerated,  $\text{N}_2$ -deaerated stagnant and stirred 2.0 M HCl solutions) showed that  $E_{\text{corr}}$  under polarization conditions is shifted to more positive values.
2.  $i_{\text{corr}}$  in case of  $\text{N}_2$ -deaerated stagnant and stirred solutions is less than that of naturally aerated solution which reflects the rate of electrochemical reactions that occurred on electrode surface, being faster in absence of  $\text{N}_2$  gas.
3. The constancy of Tafel slopes ( $b_a \approx 90\text{--}95 \text{ mV}$ ,  $b_c \approx 95 \text{ mV}$ ) under all solution states proved that the mechanistic sequences of cathodic and anodic reactions are similar.
4.  $R_p$  in naturally aerated solution is less than that in  $\text{N}_2$  deaerated stagnant and stirred solutions which reflect the nature of formed oxide layer on electrode surface being higher in naturally aerated than the other states. This agrees with that recorded in open circuit conditions ( $R_p = 30.49, 43.11, \text{ and } 41.33 \text{ } \Omega \cdot \text{cm}^2$  for naturally aerated,  $\text{N}_2$ -deaerated stagnant and stirred solutions, respectively).

### 3. Effect of Solution Temperature:

The effect of temperature on the electrochemical behavior of Sabcic mild steel in 2.0 M HCl solutions was studied using the different measurements, e.g. weight loss, open-circuit potential, EIS and potentiodynamic polarization. Fig. 9a–d shows such measurements

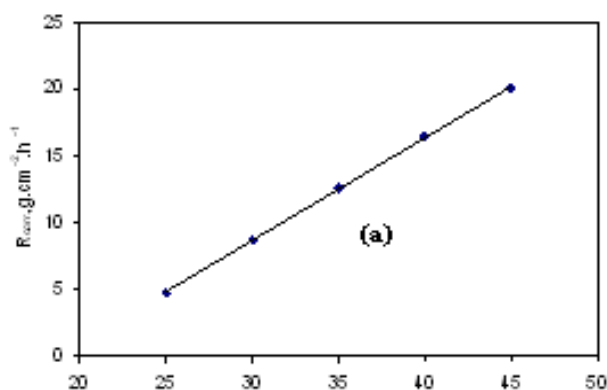
at different solution temperatures. It has been observed that the rate of electrochemical processes increased with raising solution temperature, the corrosion rate,  $R_{\text{corr}}$ , increases,  $E_{\text{ss}}$  shifts to more positive potential values, the diameter of the semicircles of the Nyquist complex plane decrease,  $E_{\text{corr}}$  increases to more positive values,  $I_{\text{corr}}$  increases and the polarization resistance,  $R_p$ , calculated from polarization parameters decreases. The fact showing the influence of such parameters with raising solution temperature was studied extensively by many authors [20–25]. In addition it is important to demonstrate the corrosive action of  $\text{Cl}^-$  ions with increasing temperature which appear as pits, especially, under polarization.

The activation energy,  $E_a$ , of the electrochemical processes can be computed from derived parameters of different measurements and presented in Fig. (10a-c). The relations are linear and obey the following equation:

$$P = A \exp(-E_a/RT)$$

Where  $P = R_{\text{corr}}, (R_p)_{\text{EIS}}, (R_p)_{\text{polarization}}$  and  $I_{\text{corr}}$

$E_a$  is the apparent activation corrosion energy under different application conditions,  $T$  is the absolute temperature,  $R$  is the universal gas constant and  $A$  is a constant depends on the type and electrolyte nature. The values of activation energy calculated are equal to 55.65, 61.87, 56.27 and 56.27  $\text{kJ} \cdot \text{mol}^{-1}$  for weight loss measurements, EIS and potentiodynamic polarization. Such values are comparable with those obtained by Elkadi *et al* [6] and Lebrini *et al* [9].



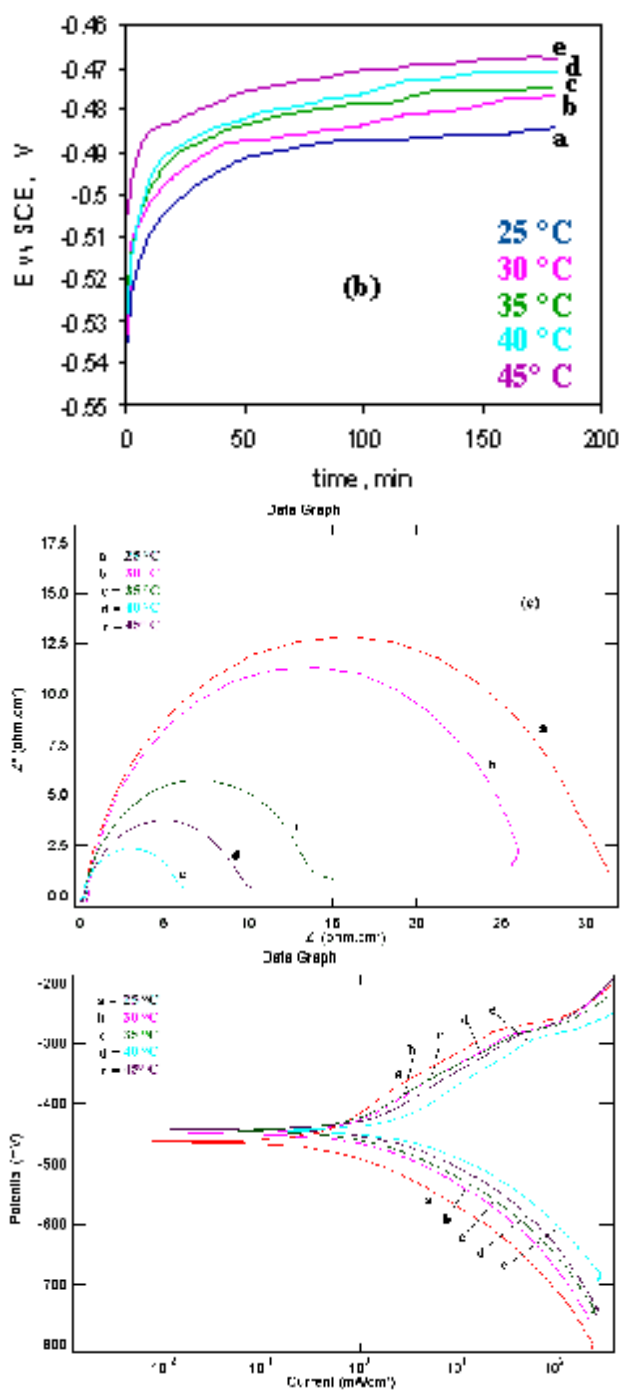
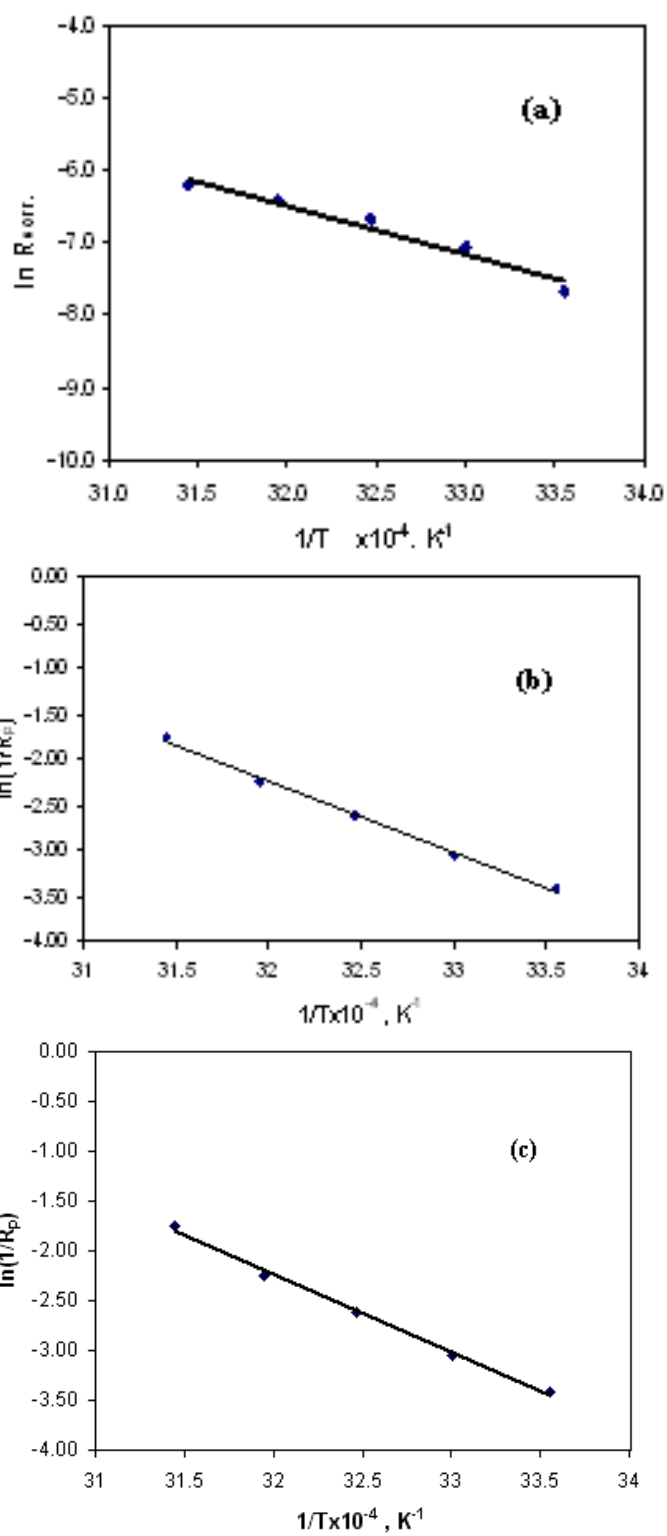
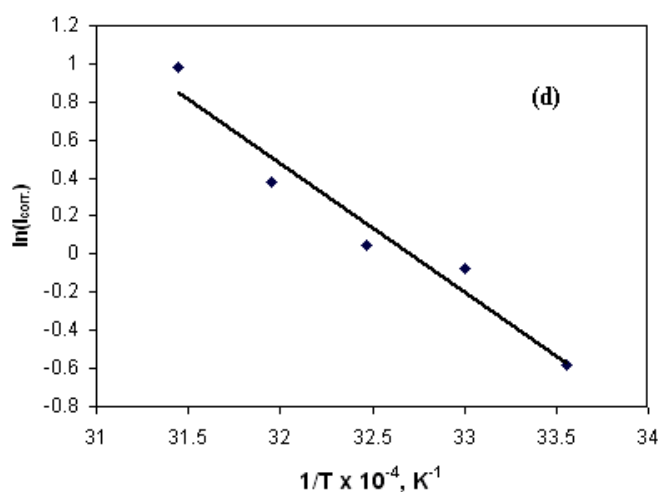


Fig. 9: Variation of corrosion rate,  $R_{corr}$ , (a) open-circuit potential,  $E$  vs SCE, (b), EIS presented in Nyquist plot (c) and potentiodynamic polarization curves (d), with temperature for Sabc mild steel in 2.0 M HCl solutions.





**Fig. 10: Arrhenius plots of  $\ln R_{corr}$  (a),  $\ln(R_p)^{-1}_{EIS}$  (b),  $\ln(R_p)^{-1}$  polarization (c) and  $\ln I_{corr}$  (d), versus reciprocal of absolute temperature, ( $T^{-1}$ ), for Sabc mild steel in 2.0 M HCl solutions.**

#### 4. Morphological Investigation:

Microstructure studies of Sabc mild steel samples of mechanically polished surface before corrosion and after corrosion process in 2.0 M HCl solutions at 25°C and 45°C were performed and illustrated in Fig. 11a-c. It is important to note that the sample surface before corrosion process is homogeneous and free from scratches and defects, cf. Fig. 11a, but after corrosion the surface state changes depending on acid concentration and solution temperature. At 25°C the sample surface is covered with gray layer containing a fine dark spots, cf. Fig. 11b, at relatively higher temperature, 45°C, the covered layer becomes compact through which the dark spots are clear and distributed non homogeneously, cf. Fig. 11c. The covered surface layer formed on Sabc mild steel sample is of oxide type resulting from anodic reactions accompanied the corrosion process [26]. So, it is important to demonstrate that presence of  $Cl^-$  ions in acid solution together with the solution temperature affect the pits and its propagation. Finally, the micrographs of sample surface seem to accord and support the results obtained by other measurements.

#### Conclusions:

The corrosion behavior of Sabc mild steel in HCl solutions was examined under different environmental factors such as acid concentration, solution temperature and state using weight loss,

open-circuit potential, EIS and potentiodynamic polarization measurements, and optical microscopy. The rate of corrosion was found to depend on acid concentration and solution temperature, it increased with increasing both the two factors from one hand and immersion time on the other hand. In the same way, the steady state potential and the  $E_{corr}$  are shifted to more positive values with increasing both the acid concentration and solution temperature, the amount of shift is relatively more under polarization conditions. Also, the corrosion current,  $I_{corr}$  increases in the same direction with acid concentration and raising the solution temperature of constant concentration. The mechanistic sequences of each of the cathodic and anodic electrochemical processes are uninfluenced with acid concentrations and solution temperature but their rates are increased with increasing both factors. On the other hand, the solution states showed a minor effect for Sabc mild steel in 2.0 M HCl under open-circuit and polarization conditions where  $E_{corr}$  is more positive than steady state potential. The main activation energy of corrosion process is equal  $\approx 57.4 \text{ kJ mol}^{-1}$  for all measurements. Morphological investigations of surface samples illustrate the corrosive action of  $Cl^-$  ions as pits, its propagation and distribution over the covered oxide film depend on HCl concentration and solution temperature.

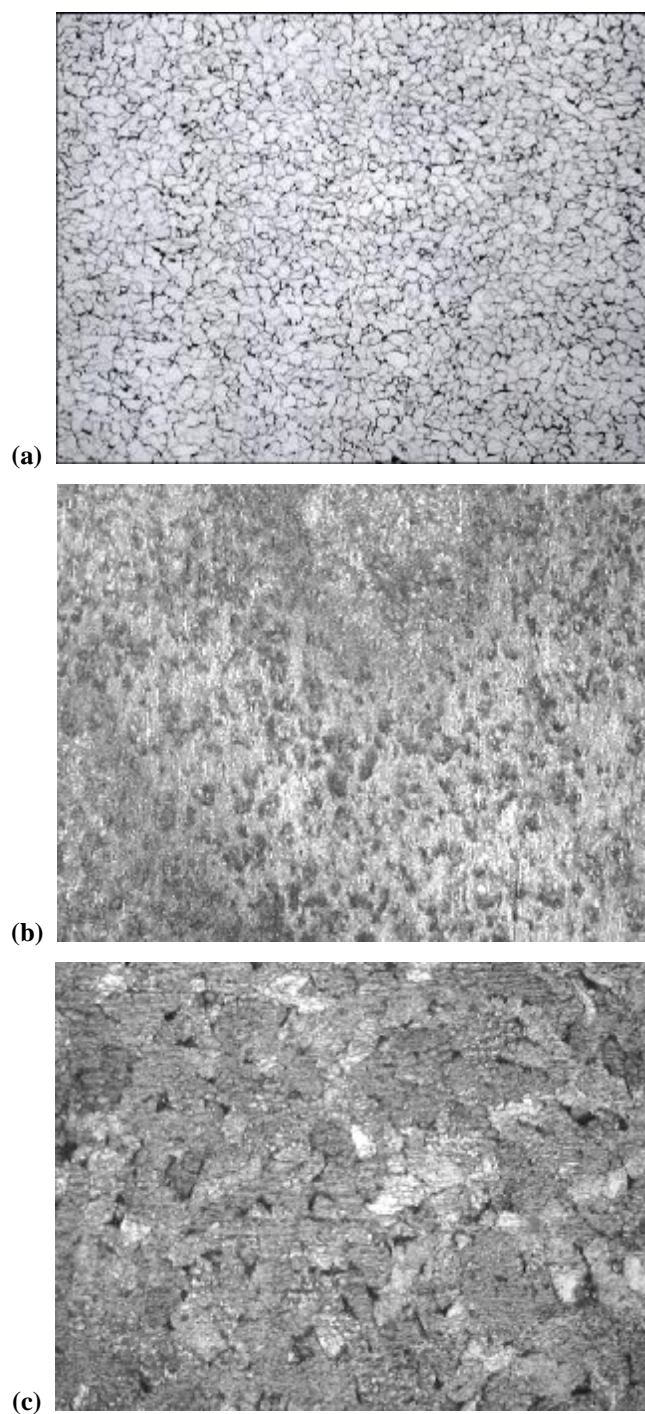


**Fig. 11: Optical micrographs of Sabic mild steel (a) mechanically polished (b) after immersion in 2.0 M HCl solution for 1hour at 25°C and 45°C(c) (500x).**

## REFERENCES

- [1] E. McCafferty and Norman Hackerman, *J. Electrochem. Soc.*, **119** (18), 999-1008 (1972).
- [2] N. Sato, T. Nada and K. Kudo, *Electrochimica Acta*, **19**, 471-475 (1974).
- [3] R.H. Hausler, *Corrosion NACE*, **42**(12), 729-739 (1986).
- [4] P. Li, T.C. Tan and J.Y. Lee, *Corros. Sci.*, **38**(11), 1935-1955 (1996).
- [5] H. Nguyen Thi Le, B. Gorcia, C. Deslouis and Q. Le Xuan, *J. of Appl. Electrochem.*, **32**(1), 105-110 (2002).
- [6] L. Elkadi, B. Mernari, M. Traisnel, F. Bentiss and M. Lagrenee, *Corros. Sci.*, **42**, 703-719 (2000).
- [7] A.E. Stoyanova and S.D. Peyerimhoff, *Electrochimica Acta*, **47**, 1365-1371(2002).
- [8] O.K. Abiola and N.C. Oforika, *Materials Chemistry and Physics*, **83**, 315-322 (2004).
- [9] M. Lebrini, M. Lagrenee, H. Vezin, L. Gengembre and F. Bentiss, *Corros. Sci.*, **47**, 485-505 (2005).
- [10] H. Schweickert, W. Lorenz and H. Friedburg, *J. Electrochem. Soc.*, **127**, 1693 (1980).
- [11] M. Keddad, O.R. Mattos and H. Takenouti, *J. Electrochem. Soc.*, **128**, 257 (1981).
- [12] S.A. Salih, A.G. Gad Allah, A.A. Mazhar and R.H. Tammam, *J. of Appl. Electrochem.*, **31**, 1103-1108 (2001).
- [13] A.G. Gad Allah, M.A. Al-Khaldi and J. Al-Ghamdi, Accepted for Publication in *JSCS*, (2006).
- [14] A.G. Gad Allah and H.M. Tamous, *B. of Electrochem.*, **11** (4), 178-187 (1995).
- [15] G. Wranglen, "An Introduction to Corrosion and Protection of Metals", Chapman and Hall, London, New York (1985).
- [16] M. Metikos-Hukovic, R. Babic, Z. Grubac and S. Brinic, *J. of Appl. Electrochem.*, **24**, 772-778 (1994).
- [17] M.W. Kendig and J. Scully, *Corrosion NACE*, **46**(1), 22-30 (1990).
- [18] L. Young, "Anodic Oxide Film", Academic Press, London, New York, p. 253 (1961).
- [19] J.O.M. Bockris and A.K.N. Reddy, "Modern Electrochemistry", Plenum Press, New York (1970).
- [20] H.J. Engell, *Electrochimica Acta*, **22**, 987-993 (1977).
- [21] I.A. Ammar and F.M. El-Khorafi, *Werkst. Korros.*, **24**, 702 (1973).
- [22] A. Atkinson and A. Marshall, *Corros. Sci.*, **18**(5), 427-439 (1978).
- [23] J. Jelinek and P. Neufeld, *Corros. Sci.*, **20**(4), 489-496 (1980).
- [24] B.E. El-Anodouli, B.G. Ateya and F.M. El-Nizamy, *Corros. Sci.*, **26**, 419-425 (1987).
- [25] A.E. Stoyanova, E.I. Sokolova and S.N. Raicheva, *Corros. Sci.*, **39**(9), 1595-1604 (1997).
- [26] D. Chebabe, Z. Aitchikh, N. Hajjaji, A. Srhiri and F. Zucchi, *Corros. Sci.*, **45**(2), 309-320 (2003).
- [27] A.G. Gad Allah, N.N. Girgis, H. Moustafa and T.F. Mikail, *H.J. of Industrial Chemistry (Veszprem)*, **23**, 11-19 (1995).
- [27] **A.G. Gad Allah,**

